Finite Elements for a Thermomechanical Analysis of Solidification Processes

Michel Bellet, Charles Aliaga, Olivier Jaouen

Finite Elements for a Thermomechanical Analysis of Solidification Processes

Michel Bellet[1], Charles Aliaga[2] and Olivier Jaouen[3]

[1] Ecole des Mines de Paris, Centre de Mise en Forme des Matériaux (CEMEF), UMR CNRS 7635, BP 207, F-06904 Sophia Antipolis, France
[2] Sciences & Computers Consultants, rue Roland Garros, F-42160 Andrézieux-Bouthéon, France
[3] Transvalor S.A., Les Espaces Delta, BP 37, F-06901 Sophia Antipolis, France

Abstract

This paper presents a thermo-mechanical approach to the numerical simulation of solidification processes. A three-dimensional finite element analysis is presented. After a brief recall about the heat transfer computation, the mechanical model is detailed. The behaviour of the cast alloy is modelled either by a thermo-elastic-viscoplastic model, or by a thermo-viscoplastic model, depending on the local solid fraction. The mould is deformable and assumed thermo-elastic. A mixed velocity-pressure formulation has been developed, using tetrahedral P1+/P1 elements. The model has been implemented in Thercast software for three-dimensional casting simulation.

Proc. MCWASP IX, 9th Int. Conf. on Modeling of Casting, Welding and Advanced Solidification Processes, Aachen (Germany), August 20-25, 2000, P.R. Sahm, P.N. Hansen and J.G. Conley (eds.), Shaker Verlag, Aachen, pp. 10-17 (2000)

1 Introduction

This paper presents the main lines of the finite element code Thercast, which aims at the three-dimensional thermomechanical analysis of castings during their solidification. The heat transfer module has been developed previously and will not be presented in the present paper, see [1]. The main issue addressed by this simulation software is the generation of deformations and stresses in cast parts, taking into account the possible deformation of the mould. It also focuses at the possible thermal convection fluid flow occurring in the regions still liquid during solidification.

The numerical code has been developed in the framework of a three-dimensional velocity-pressure finite element resolution, using tetrahedral P1+/P1 elements. This kind of formulation presents the advantage of being efficient for the computation of either liquid-like or solid-like continuous media. Depending on their temperature (and associated constitutive model), the elements are treated differently. When solid, they are treated as Lagrangian (i.e. the mesh velocity equals the material velocity) whereas when liquid they are treated as Eulerian-Lagrangian (i.e. the mesh velocity is calculated independently of the material velocity). This prevents the mesh from degenerating when fluid motion occurs in the casting, due to thermal convection. Also this allows the mesh boundary to follow the evolution of the free surface of the remaining liquid pool and then to model open shrinkage. In this paper, we will give the essential of the formulation and show an application to an actual industrial part.

2 Mechanical analysis of solidifying parts

2.1 Constitutive equations of metallic alloys

In the framework of stress computations in solidification analysis, the elastic-viscoplastic model has been widely applied to model the behaviour of metallic alloys on a very large temperature interval, including temperatures at which the alloy is liquid or mushy [2]. However, such a global model is affected by strong limitations, among which the impossibility to provide a simple and acceptable representation of liquid or mushy states. As a matter of fact, this model cannot account for natural convection in liquid regions and yields wrong volumetric shrinkage at the liquid-solid phase change because of spurious elastic deformations. Consequently, we distinguish clearly the constitutive equations for solid state and mushy or liquid states.

<u>Liquid-like constitutive equations</u>

A pure thermo-viscoplastic model is used. In this case, the compressibility is only due to the thermal contribution (no elasticity). The equations of the constitutive model can be written as follows:

$$\begin{cases} \dot{\boldsymbol{\varepsilon}} = \dot{\boldsymbol{\varepsilon}}^{vp} + \dot{\boldsymbol{\varepsilon}}^{th} \\ \dot{\boldsymbol{\varepsilon}}^{vp} = \dfrac{1}{2K}\left(\sqrt{3}\dot{\varepsilon}_{eq}\right)^{1-m}\boldsymbol{s} \\ \dot{\boldsymbol{\varepsilon}}^{th} = \left(\alpha\dot{T} + \dfrac{1}{3}\dot{g}_s\Delta\varepsilon^{tr}\right)\boldsymbol{I} \end{cases} \tag{1}$$

in which the strain rate tensor $\dot{\boldsymbol{\varepsilon}}$ is split into a viscoplastic, and a thermal part. The latter includes thermal expansion and shrinkage due to the liquid-solid phase change, $\dot{T}$ being the temperature rate, α the thermal linear expansion coefficient, $\dot{g}_s$ the rate of the volumic solid fraction, $\Delta\varepsilon^{tr}$ the relative volume change associated with the total liquid-solid transition and $\boldsymbol{I}$ the identity tensor. Equation (1b) is the classical constitutive equation of a generalized non Newtonian fluid. It relates the viscoplastic strain rate and the stress deviator $\boldsymbol{s}$, which is in turn defined by:

$$\boldsymbol{s} = \boldsymbol{\sigma} + p\boldsymbol{I} \qquad\qquad p = -\frac{1}{3}\mathrm{tr}\boldsymbol{\sigma} \tag{2}$$

in which $\boldsymbol{\sigma}$ is the Cauchy stress tensor and p the associated hydrostatic pressure. In relation (1b) K is the so-called consistency of the material and m is the strain-rate sensitivity coefficient, while $\dot{\varepsilon}_{eq}$ is the von Mises equivalent strain-rate, defined by:

$$\dot{\varepsilon}_{eq} = \sqrt{\frac{2}{3}\dot{\varepsilon}_{ij}^{vp}\dot{\varepsilon}_{ij}^{vp}} \tag{3}$$

The limit case of the Newtonian behaviour (liquid state) is obtained for m = 1. In this case, K is simply the dynamic viscosity of the fluid.

Solid-like constitutive equations

A thermo-elastic-viscoplastic model is used to represent the behaviour of the solidifying material. It is described by the following equations:

$$\begin{cases} \dot{\boldsymbol{\varepsilon}} = \dot{\boldsymbol{\varepsilon}}^{el} + \dot{\boldsymbol{\varepsilon}}^{vp} + \dot{\boldsymbol{\varepsilon}}^{th} \\ \dot{\boldsymbol{\varepsilon}}^{el} = (\boldsymbol{D}^{el})^{-1}\dot{\boldsymbol{\sigma}} = \dfrac{1+\nu}{E}\dot{\boldsymbol{\sigma}} - \dfrac{\nu}{E}\mathrm{tr}(\dot{\boldsymbol{\sigma}})\boldsymbol{I} \\ \dot{\boldsymbol{\varepsilon}}^{vp} = \dfrac{\partial Q}{\partial \boldsymbol{\sigma}} = \dfrac{\sqrt{3}}{2\sigma_{eq}}\left\langle \dfrac{\sigma_{eq} - \sigma_{00} - H\varepsilon_{eq}{}^{n}}{K\sqrt{3}} \right\rangle^{\frac{1}{m}} \boldsymbol{s} \\ \dot{\boldsymbol{\varepsilon}}^{th} = \left(\alpha\dot{T} + \dfrac{1}{3}\dot{g}_s\Delta\varepsilon^{tr}\right)\boldsymbol{I} \end{cases} \tag{4}$$

The strain rate tensor $\dot{\boldsymbol{\varepsilon}}$ is split in an elastic, a viscoplastic, and a thermal part. As in the fluid-like model, the latter includes thermal expansion and shrinkage due to the liquid-solid phase change (relation (4d) or (1c)), Equation (4b) yields the hypoelastic Hooke's law, where E is Young's modulus, ν the Poisson's coefficient, $\boldsymbol{D}^{el}$ the elasticity tensor and $\dot{\boldsymbol{\sigma}}$ a time derivative of the stress tensor. Equation (4c) gives the relation between the viscoplastic strain rate and the stress deviator $\boldsymbol{s}$, in which σ_{eq} is the von Mises equivalent stress defined by:

$$\sigma_{eq} = \sqrt{\frac{3}{2}s_{ij}s_{ij}} \tag{5}$$

In equation (4c) $\sigma_0 = \sigma_{00} + H\varepsilon_{eq}{}^{n}$ denotes the static yield stress below which no viscoplastic deformation occurs (the expression between brackets is reduced to zero when negative).

In Thercast software, all material parameters of constitutive equations can be defined pointwise as a function of temperature.

Remarks on constitutive equations

The critical temperature separating the two constitutive models can be chosen arbitrarily. If we refer to previous works dedicated to the rheological characterisation of metallic slurries [3] it seems that the limit temperature could be taken equal to the “coherency” temperature, which is defined as the temperature below which the semi-solid medium can support stresses, due to the setting up of a continuous solid skeleton. In this case, the transition temperature between the two types of constitutive models is located within the solidification interval. This means that elastic effects begin to be noticeable in the mushy state, at high solid fraction.

An alternative could be to take a transition temperature lower than the coherency temperature, possibly lower than or equal to the solidus temperature. If lower, this means that the elastic effects are considered negligible at high temperature in solid state. This is a frequent approximation in hot metal forming analysis.

It can be concluded from those considerations that there is still a great need for experimental rheological work. However, in the authors opinion, it is really necessary to separate clearly liquid-like and solid-like models in such stress-strain analysis in solidification.

It is also worth noting that in this approach the mushy zone is considered as a single phase continuous medium. In other words, we don't distinguish the velocity of the liquid phase from the velocity of the solid phase. This is clearly a simplification. It is thought that regarding stress-strain prediction, this approximation is admissible since the mushy zone probably does not play a prominent role in stress-strain development. However the conclusion would be different in the context of segregation computation. Therefore simultaneous computations of stress-strain and alloy element segregation would require more complex constitutive models.

3.2 Mechanical equilibrium equations

At any time, in any domain (the solidifying part or the mould components) the mechanical equilibrium is governed by the momentum equation:

$$\nabla.\boldsymbol{\sigma} + \rho\boldsymbol{g} - \rho\boldsymbol{\gamma} = \nabla.\boldsymbol{s} - \nabla p + \rho\boldsymbol{g} - \rho\boldsymbol{\gamma} = 0 \tag{6}$$

where $\boldsymbol{g}$ denotes the gravity vector and $\boldsymbol{\gamma}$ the acceleration vector. It should be noticed that gravity and inertia can be neglected in the mould components. The acceleration is in fact noticeable only in the liquid pools, when they are affected by fluid convection.

Mechanical boundary conditions

The part boundary $\partial\Omega_1$ can be divided into two main regions (the extension of contact boundary conditions to the interaction with deformable mould components will be explained further):

• $\partial\Omega_{1/mould}$ consists of the boundary regions $\partial\Omega_{1/j}$ of the part facing the mould components (domains Ω_j, $j \geq 2$). The unilateral contact condition is applied to these surfaces:

$$\begin{cases} \sigma\ \boldsymbol{n}.\boldsymbol{n} \leq 0 \\ \delta \geq 0 \\ (\sigma\ \boldsymbol{n}.\boldsymbol{n})\ \delta = 0 \end{cases} \tag{7}$$

where δ is the local interface gap width (positive when air gap exists effectively) and $\boldsymbol{n}$ is the local outward unit normal to the part. The fulfilment of (7) is obtained by means of a penalty condition, which consists in applying a normal stress vector proportional to the normal velocity difference via a penalty constant χ_p (the brackets in the following expression denote the positive part):

$$\boldsymbol{T} = \boldsymbol{\sigma n} = -\chi_p \left\langle (\boldsymbol{v} - \boldsymbol{v}_{mould}).\boldsymbol{n} \right\rangle \boldsymbol{n} \tag{8}$$

The tangential friction effects between part and mould are neglected.

• $\partial\Omega_{1/press}$ consists of the regions of $\partial\Omega_1$ not facing the mould, i.e. where an external fluid pressure $P_{ext}(t)$ is prescribed. This pressure can be either the atmospheric pressure, on so-called free surfaces, or a prescribed pressure due to the process itself. Consequently, locally, the external stress vector reduces to an applied normal stress vector on $\partial\Omega_{1/press}$:

$$\boldsymbol{T} = \boldsymbol{\sigma n} = -P_{ext}(t)\boldsymbol{n} \tag{9}$$

4 Numerical resolution

The primitive variables are velocity and pressure. The problem to be solved is then composed of two equations. The first one is the weak form of the momentum equation, also known as the principle of virtual work. Since p is kept as a primitive variable, only the deviatoric part of constitutive equations is accounted for and has to be solved locally in order to determine the deviatoric stress tensor $\boldsymbol{s}$. Therefore the second equation consists of a weak form of the volumetric part of the constitutive equations. It expresses the incompressibility of the plastic deformation and will govern the pressure evolution. This leads to:

$$\begin{cases} \forall \boldsymbol{v}^* \quad \int_\Omega \boldsymbol{s} : \dot{\boldsymbol{\varepsilon}}^* dV - \int_\Omega p \nabla . \boldsymbol{v}^* dV - \int_{\partial\Omega} \boldsymbol{T} . \boldsymbol{v}^* dS - \int_\Omega \rho \boldsymbol{g} . \boldsymbol{v}^* dV + \int_\Omega \rho \boldsymbol{\gamma} . \boldsymbol{v}^* dV = 0 \\ \forall p^* \quad \int_\Omega p^* \operatorname{tr} \dot{\boldsymbol{\varepsilon}}^{vp} dV = 0 \end{cases} \tag{10}$$

The pressure variable appears as a Lagrange multiplier of the plastic incompressibility constraint. The term integrated in the second equation will change according to the local state of the alloy (i.e. according to the local temperature). It can be generally written:

$$\operatorname{tr} \dot{\boldsymbol{\varepsilon}}^{vp} = \operatorname{tr} \dot{\boldsymbol{\varepsilon}} - \operatorname{tr} \dot{\boldsymbol{\varepsilon}}^{el} - \operatorname{tr} \dot{\boldsymbol{\varepsilon}}^{th} = \nabla . \boldsymbol{v} + \frac{3(1-2\nu)}{E} \dot{p} - 3\alpha \dot{T} - \dot{g}_s \Delta \varepsilon^{tr} \tag{11}$$

but in case of a liquid-like constitutive equation (pure viscoplastic behaviour), the elastic contribution will vanish. Accordingly, the stress deviator $\boldsymbol{s}$ in (10a) will result either from an elastic-viscoplastic constitutive equation, or from a viscoplastic or Newtonian law.

The time and space discretization will not be recalled here: see references [4, 5]. The formulation permits to treat simultaneously the solidified zones and the liquid or mushy pools of a casting. The contribution of each finite element to (10) is computed considering either a viscoplastic or an elastic-viscoplastic constitutive model, depending on the temperature at the centre of the element.

A Eulerian-Lagrangian formulation has been developed [4, 5], in order to account for the fluid flow occurring in the liquid regions. Depending on the size of the part, the melt can be put into motion by thermal convection. In such regions, the finite element mesh remains quasi static (following the motion of the free surface due to the contraction of the alloy). This gives rise to advection terms in the equations, which are taken into account by an original nodal upwind formulation.

4.1 Mechanical coupling algorithm for part-mould and mould-mould interactions

The objective is to model mould deformation and contact interactions occurring either between the cast part and the mould components or between the mould components themselves. In a first approach, the mould components are assumed thermo-elastic, obeying the Hooke's linear law. This problem of contact between several deformable bodies is modelled by means of the penalty approach.

In practice, along an interface between two domains *A* and *B*, we chose arbitrarily to penalize the penetration of *A* into *B*, which means that in the resolution of the mechanical equilibrium of *A*, the following penalty term is added:

$$\int_{\partial\Omega_{AB}} -\chi_p \left\langle (\boldsymbol{v}^A - \boldsymbol{v}^B) . \boldsymbol{n} \right\rangle \boldsymbol{n} . \boldsymbol{v}^* dS \tag{12}$$

where $\boldsymbol{v}^A$ and $\boldsymbol{v}^B$ are the respective local velocities of the two domains, $\boldsymbol{n}$ being the normal at interface and χ_p the penalty coefficient. Accordingly, considering the action-reaction principle, the following normal stress vector $\boldsymbol{T}$ is applied to the surface of *B*:

$$\boldsymbol{T} = \chi_p \left\langle (\boldsymbol{v}^A - \boldsymbol{v}^B).\boldsymbol{n} \right\rangle \boldsymbol{n} \quad (13)$$

During the simulation of a solidification process, the equilibrium of each domain with respect to its neighbouring domains is computed. Since the cooling is generally not very rapid, there is no need to solve simultaneously the equilibrium of all the bodies (this would be obtained by a heavy and costly fix point procedure or by a global computation including all domains). A staggered scheme is preferred, each domain being calculated only once per increment.

5 Application: automobile braking disk

Such a formulation has been first validated by comparison to simple instrumented tests: see [4, 5]. We present here its application to a more complex industrial case. The part is a ventilated braking disk for automobile, made of grey iron. The mould and the internal core are made of sand (fig. 1). The objective of the finite element analysis is to identify the possible causes of the residual deformation of the cast part. Disks often suffer from warpage, and it has been observed experimentally that this is caused by the deformation of the central core. Each domain is meshed automatically using Thercast preprocessors. The total discretisation comprises around 100 000 nodes and 500 000 tetrahedra. An example of the finite element mesh is given at fig. 2 where the discretisation of the central core is shown.

As a first approximation, the sand is modelled using a thermo-elastic constitutive equation. On fig. 3 and 4, we can see the result of the multidomain finite element heat transfer analysis. Fig. 3 illustrates the influence of mould filling. When the initial temperatures are not taken uniform, but computed by a mould filling simulation code (in this case, Simulor), the cooling curves are modified. It can be noted that the cooling is also less uniform throughout the casting.

The material velocity field, which is caused here by solidification shrinkage, is shown on fig. 5. It can be seen that there is quite an important liquid feeding through the feeding channel and the gate before they are frozen. Such a liquid feeding can be computed thanks to the liquid-like formulation and the Eulerian-Lagrangian scheme.

As the temperature of the part decreases, it is submitted to deformations and stresses. Fig. 6 shows the air gap distribution between the part and the core. The core deforms as well, essentially because of non homogeneous heating. Fig. 7 shows the resulting distorsion of the core, which affects also the part.

6 Conclusion

The 3D finite element software Thercast is a numerical simulation tool for the analysis of the thermomechanical phenomena associated with solidification of castings. It is expected that such strain-stress thermomechanical computations will lead in a near future to accurate prediction of residual stresses and strains, hot tearing and shrinkage defects, and will contribute to a faster development and an improved quality of castings.

References

[1] M. Bellet, F. Decultieux, M. Ménaï, F. Bay, C. Levaillant, J.L. Chenot, P. Schmidt and I.L. Svensson, Thermomechanics of the cooling stage in casting processes : 3D finite element analysis and experimental validation, Met. Trans., 27B, 81-100 (1996)

[2] B.G. Thomas and C. Beckermann (eds.), Proc. 8th Int. Conf. on Modelling of Casting, Welding and Advanced Solidification Processes, San Diego, The Minerals Metals and Materials Society (1998)

[3] P. Vicente-Hernandez, Caractérisation rhéologique et microstructurale d'alliages métalliques à l'état semi-solide, PhD Thesis (in french), Ecole des Mines de Paris (1994)

[4] O. Jaouen, Modélisation tridimensionnelle par éléments finis pour l'analyse thermomécanique du refroidissement des pièces coulées, PhD Thesis (in french), Ecole des Mines de Paris (1998)

[5] M. Bellet, O. Jaouen, Finite element approach of thermomechanics of solidification processes, Proc. Int. Conf. On Cutting Edge of Computer Simulation of Solidification and Casting, Osaka (Japan), November 14-16, 1999, I. Ohnaka and H. Yasuda (eds.), The Iron and Steel Institute of Japan (ISIJ), 173-190 (1999)

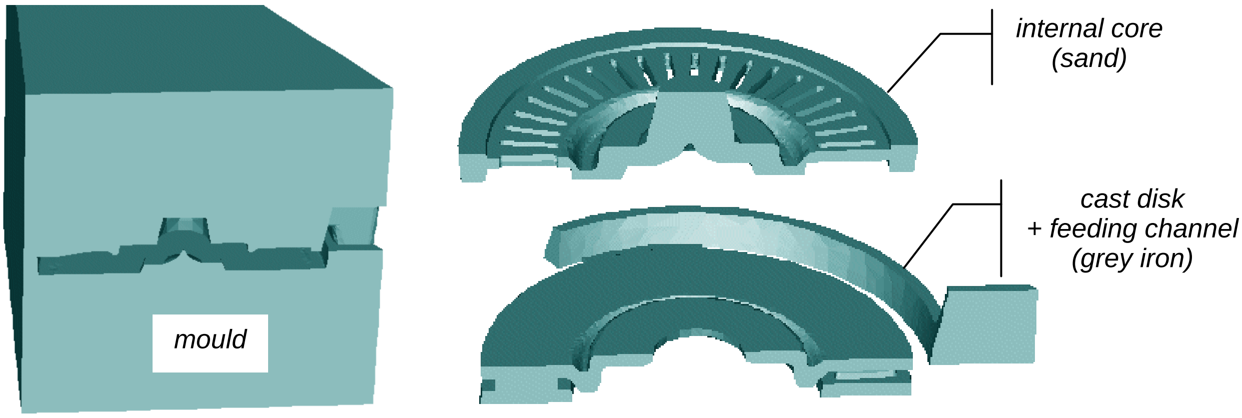

Figure 1: Sand casting of a braking disk: view of the three mould components (lower and upper mould, internal core) and of the cast part. Each domain is meshed with tetrahedral finite elements.

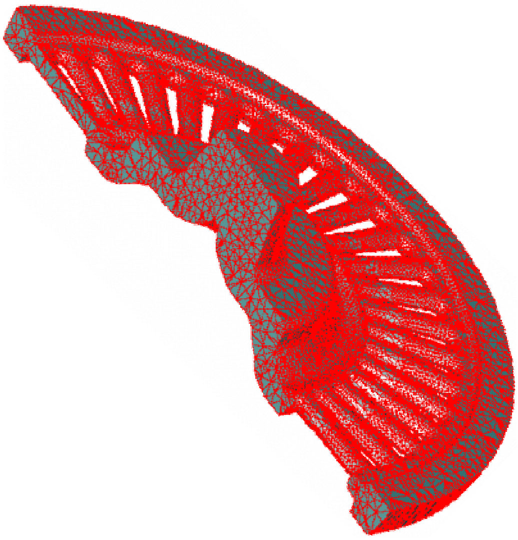

Figure 2: Mesh of the internal core.

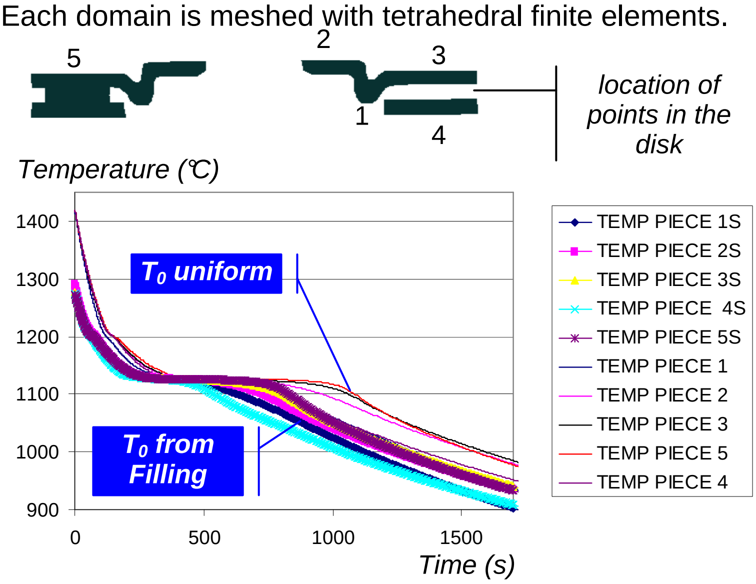

Figure 3: Cooling curves in five points of the part.

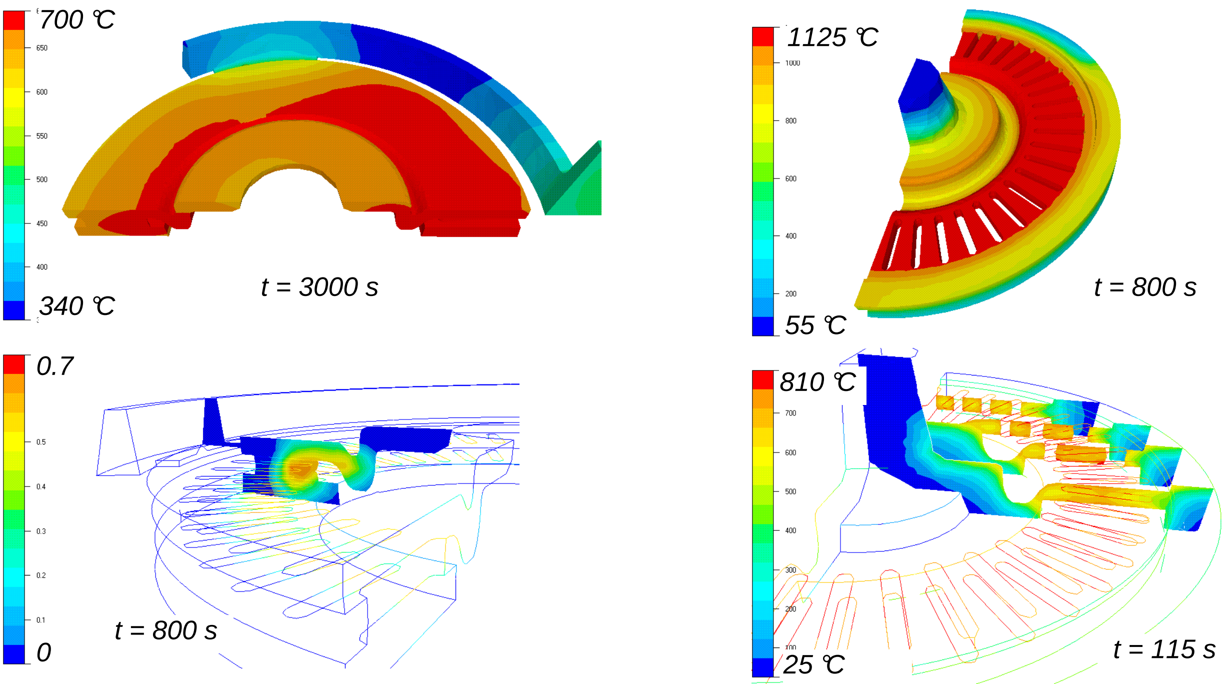

Figure 4: Heat transfer analysis. Left: temperature distribution in the disk (top) and liquid fraction in a section (bottom). Right: temperature profile in the core.

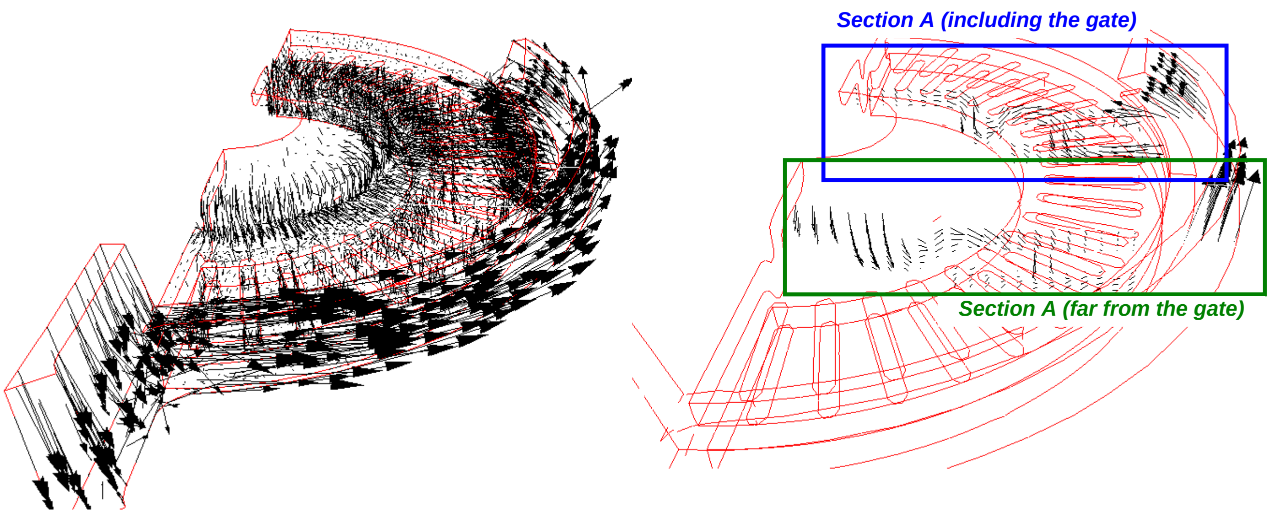

Figure 5: Material velocity field, showing liquid feeding through the gate.

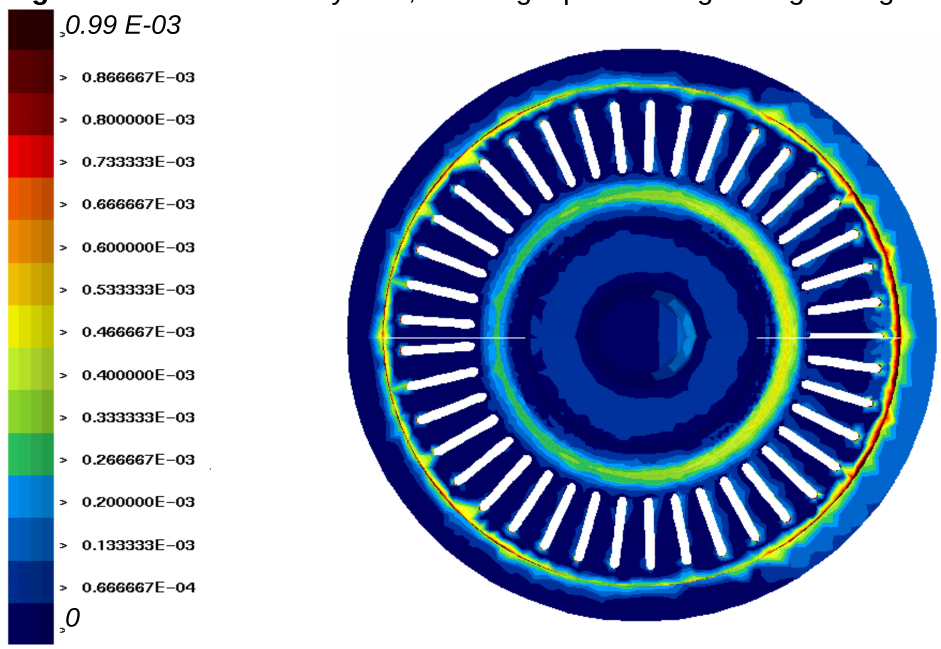

Figure 6: Air gap distribution (m), projected onto core surface.

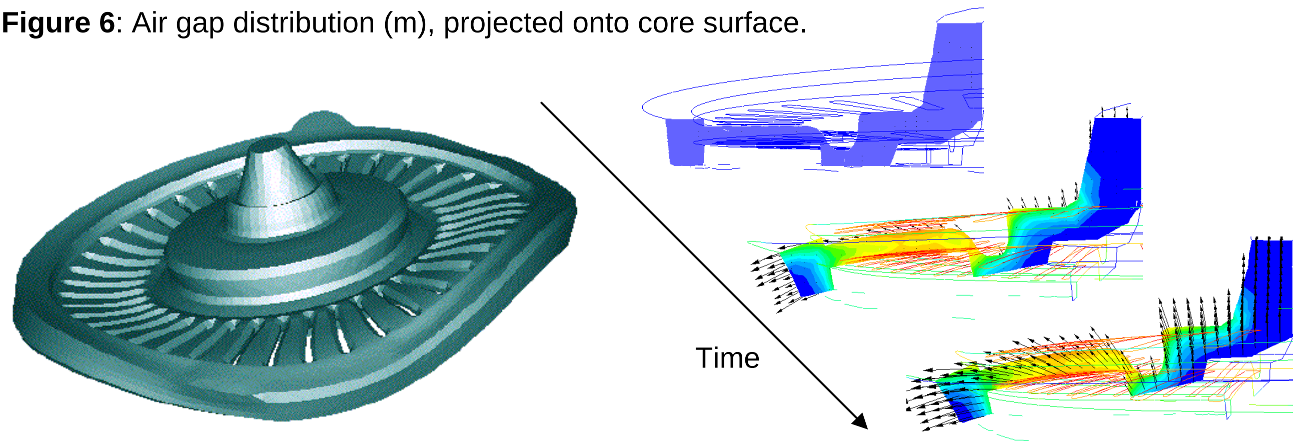

Figure 7: Deformation of the internal core (displacements magnified).

Acknowledgement

This work has been supported by the french Ministry of Industry, the Centre Technique des Industries de la Fonderie, Aubert et Duval, Creusot-Loire Industrie and Ascometal (Usinor Group), PSA Peugeot Citroën.